Available online at www.sciencedirect.com

Food and Bioproducts Processing

journal homepage: www.elsevier.com/locate/fbp

Biosynthesis of antioxidant xanthan gum by *Xanthomonas campestris* using substrates added with moist olive pomace

P.J.L. Crugeira[a,b,*], H.H.S. Almeida[a,b], I. Marcet[c], M. Rendueles[c], M.G. Pires[a,b], H.M. Rafael[a,b], A.I.G. Rodrigues[a,b], A. Santamaria-Echart[a,b], M.F. Barreiro[a,b,*]

[a] Centro de Investigação de Montanha (CIMO), Instituto Politécnico de Bragança, Campus de Santa Apolónia, Bragança, Portugal

[b] Laboratório Associado para a Sustentabilidade e Tecnologia em Regiões de Montanha (SusTEC), Instituto Politécnico de Bragança, Campus de Santa Apolónia, Bragança, Portugal

[c] Department of Chemical and Environmental Engineering, University of Oviedo, C/ Julián Clavería 8, Oviedo, Spain

ARTICLE INFO

Article history:
Received 11 July 2023
Received in revised form 20 August 2023
Accepted 21 August 2023
Available online 24 August 2023

Keywords:
Moist olive pomace
Xanthan gum
Antioxidant activity
Bacterial stress
Circular economy

ABSTRACT

Moist olive pomace (MOP) is a high moisture content by-product of the olive oil industry. Managing this recalcitrant residue (transport, storage, and drying) is a priority demanding investment in finding alternative valorisation routes. In this context, the biosynthesis of xanthan gum (XG) incorporating MOP in the substrate (0.0 %, 5.0 %, 10.0 %, 15.0 %, 20.0 %, 25.0 %, 30.0 % and 50.0 %) to induce bacterial stress was attempted. XG biosynthesis yield was quantified, and the product was characterised by structural analysis (FTIR), thermal behaviour (TG), rheology and antioxidant capacity. Relative to the control (sample with no added MOP), a significant increase in XG biosynthesis was found for concentrations up to 30.0 % MOP. In particular, for XG produced with 15 % MOP, a 50.91 % ($p < 0.0001$) increase was achieved, together with 395.78 % for viscosity. In general, XG produced with MOP presence showed antioxidant activity, a value-added property, especially for applications in the food, pharmaceutical and cosmetic areas. The results indicated that the stress imposed by the MOP induced a microbial response leading to XG production increase, structural and viscosity modifications, and antioxidant properties incorporation. Overall, this work points out a new MOP application contributing to the sustainability of the olive oil productive chain from a biobased circular economy perspective.

* Corresponding authors at: Centro de Investigação de Montanha (CIMO), Instituto Politécnico de Bragança, Campus de Santa Apolónia, Bragança, Portugal
E-mail addresses: pedro.crugeira@ipb.pt (P.J.L. Crugeira), barreiro@ipb.pt (M.F. Barreiro).

https://doi.org/10.1016/j.fbp.2023.08.008

1. Introduction

The olive oil industry is a sector that generates large amounts of by-products. Environmental and technological restructuration of the olive oil extraction units led to the adoption of centrifugation systems, particularly the so-called two-phase extraction systems, which generate large amounts of moist olive pomace (MOP). This by-product is characterised by a high moisture content and low viscosity, challenging its transport, storage and drying, resulting in low commercial value (Medeiros et al., 2016; Muscolo et al., 2019).It contains phenolic compounds such as oleuropein, hydroxytyrosol and tyrosol with antioxidant capacity and consequent prevention or inhibition of oxidative reactions in biomolecules (Rueda et al., 2023). In this scenario, MOP valorisation is fundamental, introducing this residue in the production chain, and generating sustainable value-added products.

Substrates of different compositions and various contents have been tested to reduce costs and make the biosynthesis of xanthan gum (XG) profitable. Given the growing market and application versatility of XG as a thickener, emulsifier, stabiliser and suspension agent, studies have been developed using alternative carbon sources, promoting the introduction of agro-industrial residues in its production route (Bhat et al., 2022; Demirci et al., 2019). Thus, to achieve an economically green synthesis, several substrates have been evaluated, such as sugarcane molasses, whey (Silva et al., 2009), kitchen waste (Li et al., 2016), olive mill wastewaters (López et al., 2001), tapioca pulp (Gunasekar et al., 2014), and orange peels (Mohsin et al., 2018), among others.

Excretion of exopolysaccharides by bacteria of the genus *Xanthomonas* spp. is a protective response to adverse and unfavourable conditions to increase its environmental adaptability, often promoting its adherence through forming biofilms and symbiotic relationships (Bianco et al., 2016). One of the stress forms is exposure to toxic compounds capable of developing a metabolic imbalance and consequent cellular response, inducing the activation of metabolic pathways. Examples include the Entner-Doudoroff pathway, which catabolises available glucose by about 80 % into pyruvate, directing it to the tricarboxylic acid cycle, with the remaining glucose metabolised via the pentose-phosphate pathway (Hahn et al., 2022; Hublik, 2012).

In structural terms, XG is a heteropolysaccharide composed of long polysaccharide chains. A main chain formed by D-glucose molecules, and trisaccharide side chains with two D-mannose molecules interspersed with one D-glucuronic acid molecule. The internal mannose is acetylated (acetic acid ester – acetyl-mannose), and approximately half of the terminal mannoses contain pyruvic acid, remaining pyruvyl-mannose (García-Ochoa et al., 2000). Intra and intermolecular interactions of the molecule can be affected by the proportion of the acetyl and pyruvate substituent groups, resulting in chains of different sizes and molecular weight, thus interfering in gum viscosity (Papagiannopoulos et al., 2016; Pinheiro et al., 2020).

In addition to the unique rheological properties, XG can change its molecular structure during production, influencing its intrinsic properties. Acetate or pyruvate content variations commonly depend on the production strain and growing conditions; e.g., using cations during biosynthesis strongly influences the properties of the obtained gum (e.g., synergism with galactomannans) (Ciesielski and Tomasik, 2008; Hublik, 2012). Moreover, studies carried out by Ramos de Souza et al. (2022) demonstrated the production of XG in the presence of waste residue substrates, namely water containing Zn and Fe atoms, and crude glycerin, which resulted in a polymer with thermoviscosifying behaviour holding high oil recovery yield capacity.

Antioxidant additives play a key role in food and pharmaceutical applications, preventing damage from oxidative stress generated by free radicals related to diseases such as cancer, cardiovascular disease, diabetes, and ageing (Li et al., 2007; Sarangarajan et al., 2017). Modifications in the structure of XG have been carried out to potentiate its antioxidant activity, such as the partial hydrolysis of the exopolysaccharide, increasing the number of hydroxyls or the transformation of the polysaccharide into a sodium salt, where the oxidation reaction ends up transforming the OH groups into $NaOO^{-}$ ones (Delattre et al., 2015; Xiong et al., 2014).

This work aimed to evaluate the biosynthesis of XG by *Xanthomonas campestris* using substrates added with MOP. Different MOP concentrations were evaluated to induce bacterial stress capable of triggering a cellular response with the potential to increase the production of value-added gum, which were evaluated concerning structural analysis (FTIR), thermal behaviour (TG), rheology and antioxidant capacity. To the best of our knowledge, the synthesis of XG with antioxidant properties using biosynthesis, particularly in the presence of MOP, has yet to be reported so far.

2. Materials and methods

2.1. Moist olive pomace samples

The MOP was collected at the olive oil extraction unit Olimontes (Macedo de Cavaleiros, Portugal), operating using a continuous two-phase centrifugation system. The samples were pasteurised at 60 °C for 30 min (Ecoline 012, Lauda, Königshofen, Germany) and cooled to 4 °C for storage (H8 A1E W, Hotpoint-Ariston, Lisbon, Portugal) until use.

2.2. Moist olive pomace phenolic compounds profile analysis

High-performance liquid chromatography (HPLC) with a Diode Array Detector (DAD) was used to obtain the MOP phenolic compounds profile. Before analysis, MOP was frozen and freeze-dried (Coolsafe 110–4, Scanvac, Olsztyn, Poland), then subjected to extraction with methanol (MeOH). For that, 1.5 g of freeze-dried MOP were mixed with 50 mL, left under stirring for 1 h in the dark and filtered, followed by MeOH evaporation in a rotary evaporator at 35 °C (RE300DB, Stuart Stone, UK). Then, 5 mL of MeOH were added to the dried sample obtaining a concentration of 0.1 mg/mL, filtrated with a Whatman Nylon (0.20 µm) filter and stored in dark flasks. This procedure was repeated 3 times to achieve 3 independent trials. 20 µL were injected using an analytical HPLC Knauer Smartline apparatus equipped with a Knauer Smartline Autosampler 3800, a cooling system set to 4 °C, and Knauer DAD. A reversed-phase Shperisorb ODS2 column was used (250 ×4 mm id, 5 µm particle diameter, end-capped Nucleosil C18 (Macherey-Nagel) maintained at 30 °C. Chromatographic separation was carried out using a gradient of solvent A (water: formic acid (99.8:0.2 (v/v))) and B (MeOH), applied at a flow rate of 0.9 mL/min, as follows: 5 % B at 0 min, 15 % B at 3 min, 25 % B at 13 min, 30 % B at 25 min, 35 % B at 35 min, 40 % B at 39 min, 45 % B at 42 min, 45 % B at

45 min, 47 % B at 50 min, 48 % B at 60 min, 50 % B at 64 min and 100 % B at 66 min, 5 % B at 70 min and 5 % B at 75 min. Spectral data from all peaks were accumulated in the 200–600 nm range, and chromatograms were recorded at 254, 280, 320, and 330 nm. The compounds in each extract were identified by comparing their retention times and UV-Vis spectra with standards analysed under the same conditions and using the spectra library previously compiled by the authors. All analyses were performed in triplicate.

2.3. Microorganism and inoculum preparation

A cryogenic tube of *Xanthomonas campestris pv. Campestris* strain, ATCC 33913 (DSMZ, Braunschweig, Germany), was inoculated in 18 mL of yeast malt broth (YM) (w/v): 0.3 % yeast extract; 0.3 % malt extract; 0.5 % peptone; 1.0 % glucose (Sigma-Aldrich, Steinheim am Albuch, Germany), and the pH was adjusted to 7.0, to be incubated for 14 h at 25 °C under 150 rpm in an orbital shaking (Shel Lab, Sheldon- SI4, Cornelius, USA). Subsequently, 10 % (v/v) of the pre-inoculum was added to the YM medium. After 12 h of incubation at 25 °C and 150 rpm, the bacterial culture was ready for inoculation in the XG production process.

2.4. Xanthan gum production and extraction

The XG production medium was prepared using an inorganic constituents-based mineral salt medium (MSM) (Sampaio et al., 2022) supplemented with 2.5 % sucrose and 0.05 % yeast extract, diluted in distilled water. The pH was adjusted to 7.0 with a 5 M NaOH solution, for a final volume of 1.0 L. For the preparation of the medium containing the MOP by-products, different concentrations (w/v) were added during its preparation (5.0 %, 10.0 %, 15.0 %, 20.0 %, 25.0 %, 30 %, and 50 %).

The XG production experiments were carried out in triplicate using 250 mL Erlenmeyer flasks containing 45 mL of the production medium and 5 mL of the inoculum (10 % of the final volume), subjected to 250 rpm orbital shaking at 28 °C (Shel Lab, Sheldon- SI4, Cornelius, EUA) for 76 h. This time was defined after preliminary studies (48, 76 and 96 h) pointed out the need to use 76 h to achieve the highest productive levels. After the production, the samples were centrifuged at 10,000 g for 30 min at 4 °C (centrifuge 5810 R, Eppendorf, Hamburg, Germany) to remove the biomass and MOP impurities. The supernatant was added to 99.5 % of ethyl alcohol at 4 °C using a supernatant/alcohol ratio of 1:3 (v/v), followed by conditioning at 4 °C for 18 h for XG precipitation. The precipitated biopolymer was recovered by centrifugation (10,000 g for 30 min at 4 °C) and dried in an oven at 30 °C (ED115, Binder, Tuttlingen, Germany) until constant weight. The production yield quantification was performed by gravimetry in an analytical balance (AS 60/220. R2 Plus, Radwag, Radom, Poland).

2.5. Xanthan gum characterisation

2.5.1. Fourier transform infrared spectroscopy (FTIR)

Structural analysis of the produced XG was carried out using an MB300 FTIR from ABB (Zurich, Switzerland) operating in transmittance mode. The spectra were obtained between 4000 and 500 cm^{-1} by averaging 32 scans at a resolution of 4 cm^{-1}. Samples (1 %, w/w) were dispersed in KBr (spectroscopic grade) and pelletised before analysis. The data were acquired and treated using the Horizon MB v.3.4 software.

2.5.2. Thermogravimetric analysis (TGA)

The thermal stability of XG was analysed in a NETZSCH equipment (TG 209 F3 Tarsus, Selb, Germany). The exopolysaccharides were heated from 30° to 600°C, at 10 °C/min in alumina crucibles (6–8 mg) under an oxidative atmosphere (air) with a 50 mL/min flow rate.

2.5.3. Rheological behaviour

Flow curves were obtained using a Haake MARS II rotational rheometer equipped with a PP35s probe and a Peltier unit to control the temperature. Previously to analysis, the lyophilised XG samples were solubilised in water (1 mg/mL) at 37 °C and placed between the plate/plate with a gap of 1 mm (any sample excess was removed before testing). All the samples were stabilised for 15 min before the measurement to relax the stress and guarantee 20 ± 0.1 °C. In a steady state, the apparent viscosity of the XG solutions was obtained varying the shear rate from 0.01 1/s to 300 1/s in 360 s. The obtained data were adjusted to the Ostwald-de Waele model, Eq. 1 (da Silva et al., 2018).

$$\eta = K\dot{\gamma}^{n-1} \quad (1)$$

where η is the apparent viscosity, $\dot{\gamma}$ is the shear rate, K (Pa.s^n) is the consistency index, and n is the flow behaviour index (dimensionless). Ostwald de Waele model parameters were calculated from the obtained curves using the Haake Rheowin Software.

2.6. Antioxidant activity

$ABTS^{\cdot+}$ (2,2´-azinobis-(–3-ethylbenzothiazoline-6-sulfonic acid) radical scavenging capacity of the samples was calculated according to a modified method described by Yang et al. (2020). An initial stock solution of ABTS (Sigma-Aldrich, Steinheim am Albuch, Germany), composed of an aqueous solution of 7 mM $ABTS^{\cdot+}$ and 2.45 mM potassium persulfate, was prepared. This stock solution was kept in darkness at room temperature for 16 h before use, then diluted with distilled water up to an absorbance of 0.70 ± 0.04 at 734 nm read in a 1 cm cuvette. The samples were dissolved in water at 1 mg/mL, and aliquots of 100 µL were mixed with 4900 µL of the $ABTS^{\cdot+}$ solution and incubated in darkness at room temperature for 20 min. Finally, the absorbance of the samples was measured at 734 nm (V-730 UV–visible, Jasco, Madrid, Spain), and the scavenging capacity percentage (SC) was calculated using the following Eq. 2:

$$SC(\%) = \frac{A_r - A_t}{A_r} \times 100 \quad (2)$$

where A_t is the absorbance of the sample and A_r is the absorbance of the negative control (distilled water).

2.7. Statistical analysis

The results obtained in the different tests were analysed using ANOVA statistical test with Tukey's multiple comparison post-test using the GraphPad Prism® 8.0 software (San Diego-CA, USA).

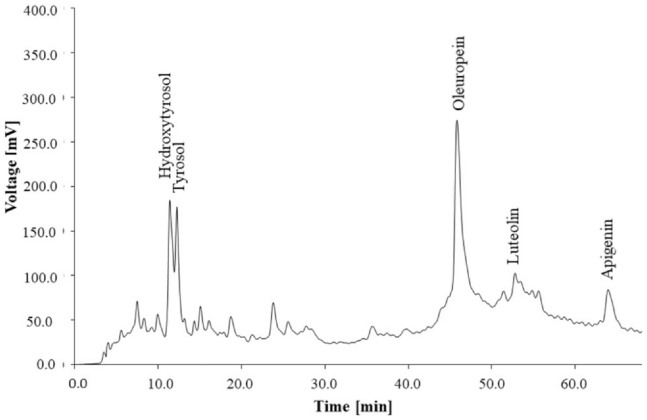

Fig. 1 – HPLC-DAD chromatogram of MOP acquired at 280 nm. Identified compounds: hydroxytyrosol, tyrosol, oleuropein, luteolin, and apigenin.

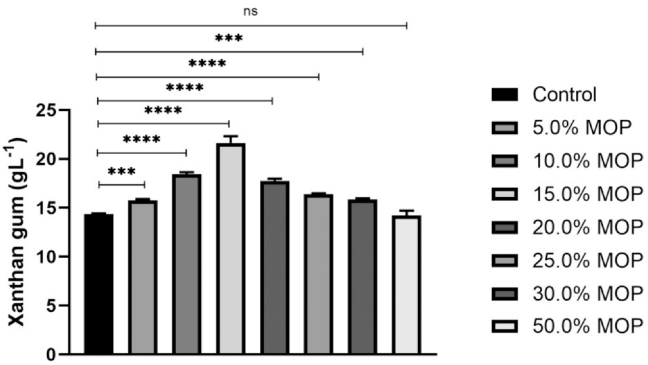

Fig. 2 – Xanthan gum production according to the studied groups. ***p < 0.001; ****p < 0.0001; ns = not significant.

3. Results and discussion

3.1. *Moist olive pomace phenolic compounds characterisation*

The MOP phenolic compound profile analysed using reversed phase-HPLC is presented in Fig. 1 Phenolic compounds with a total phenolic content (TPC) of 18315 mg/kg GAE (gallic acid equivalent) were identified as belonging to three classes: secoiridoids (oleuropein), comprising circa 78 % of TPC, followed by phenolic alcohols (hydroxytyrosol, and tyrosol) around 19 % of TPC, and flavonoids (luteolin and apigenin) at lower concentration (≈ 2 % of TPC).

To extract phenolic compounds from the olive pomace, Böhmer-Maas et al. (2020) used different aqueous methanol solutions at predetermined concentrations. TPC concentrations ranged from 20886.2 to 23061.2 mg/kg GAE in different olive pomace extracts, slightly higher than the results obtained in this work. For all the studied olive pomace extracts, Cioffi et al. (2010), observed that the secoiridoids (oleuropein and ligstroside aglycone) corresponded to the highest fraction of the TPC followed by the phenolic alcohols (hydroxytyrosol and tyrosol), in accordance with the MOP characterised in this work. The authors also identified gallic, caffeic, ferulic, and vanillic acid compounds. It is known that the phenolic compounds profile of olive pomace is influenced by the chemical composition of the olive oil, which depends on several factors, including olive cultivar, geographic origin, irrigation technique, and the extraction method (Dabbou et al., 2011, Malheiro et al., 2015, Zhang et al., 2022).

3.2. *Xanthan gum production*

The XG production yield was calculated, and the results are summarised in Fig. 2 In general, it was observed that the addition of MOP (up to 30 %) significantly increased the XG production. The highest level of biosynthesis was obtained at 15.0 % of MOP (21.64 g/L), implying an increment of 50.91 % ($p < 0.0001$) relative to the control (14.34 g/L). The results indicated that the stress imposed by the phenolic compounds, induced the protection mechanism of the bacteria against adverse conditions, consequently increasing the XG production. To evidence that even only a progressive decrease in the production was observed from 15.0 % to 30.0 % MOP (21.64, 17.74, 16.41, and 15.84 g/L), it was still statistically significant compared to the control.

This progressive reduction at concentrations higher than 15.0 % MOP is related to the antimicrobial activity of the lipophilic phenolic compounds (oleuropein, hydroxytyrosol and tyrosol) and their ability to destabilise cell membranes, as previously reported (Casadey et al., 2021; Khemakhem et al., 2018; Pannucci et al., 2021). Additionally, the phenolic compounds can unbalance the bacterial "quorum sensing" system, reducing their ability to adapt to the bacterial production stimulus, namely the MOP-modified medium (Gutierrez et al., 2009; Adonizio et al., 2006).

Studies carried out by Trindade et al. (2018) evaluated the impact of alkaline stress on *X. campestris pv. mangiferaeindicae* IBSBF 1230 population during XG biosynthesis, using crude glycerol as substrate, achieving a production increase of 73.69 %, while a decrease in the viscosity was observed (60 cP).

In this work, XG biosynthesis, using 50.0 % of MOP (14.22 g/L), reduced the production relative to the control by circa 0.84 %. In fact, no significant difference was observed between both groups, indicating that even under these conditions, MOP can be used to potentiate a circular economy strategy to obtain a value-added product, as later discussed concerning the antioxidant potential of the obtained products.

Some published works that evaluated alternative substrates to produce XG, corroborate that achieving efficient production rates is a real challenge. Silva et al. (2015) reported that coconut husk when applied as a substrate for *X. campestris pv. campestris* 2149, reached a modest production of 5.16 g/L, employing an orbital agitation of 250 rpm at 28 °C for 120 h. De M. Diniz et al. (2012) with cocoa husk as the production medium substrate, using *X. campestris pv. manihotis* 1182, *X. campestris pv. campestris* 472 and *X. campestris pv. malvacearum* 1779 strains, achieved, respectively, yields of 7.34, 0.65 and 3.45 g/L, in orbital shaking at 250 rpm, and 28 °C for 120 h. To highlight is the production of 26.42 g/L using cheese whey during 72 h, at 28 °C and 180 rpm with *X. campestris pv. manihotis* 1182 strain (Silva et al., 2009), and the production of 36 g/L (in a bench bioreactor) using the conditions of 72 h at 28 °C and 390 rpm with the *X. campestris pv. mangiferae* 1230 strain (Mesomo et al., 2009). In this work, the yields achieved are among the highest, considering similar biosynthesis times and recalcitrant alternative substrates. Even though sucrose supplementation can have favoured XG production, a clear positive effect of adding MOP to the base sucrose-supplemented medium was observed, justifying that important production levels were achieved following this strategy.

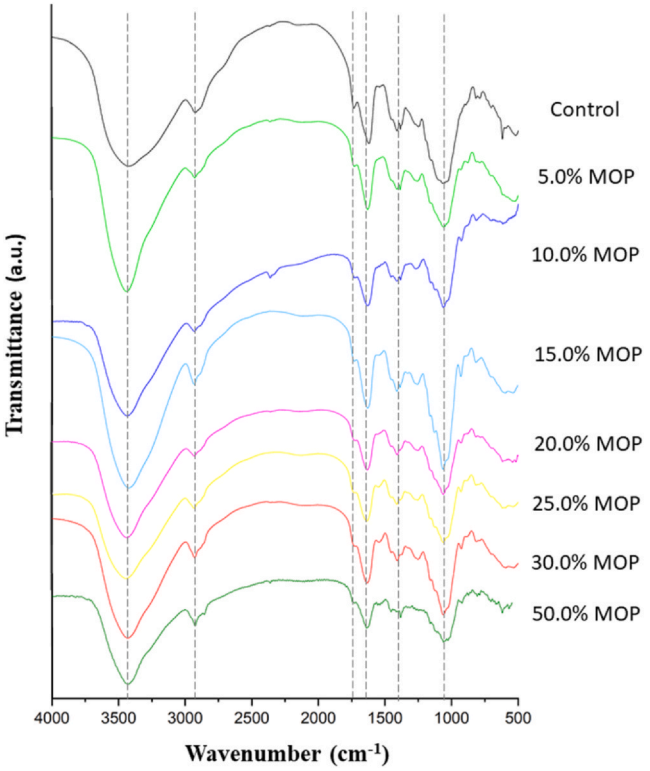

Fig. 3 – FTIR spectra of the produced biopolymers with different concentrations of MOP.

3.3. *Xanthan gum characterisation*

3.3.1. *FTIR spectroscopy*

The FTIR spectra of the produced biopolymers, presented in Fig. 3, put in evidence the characteristic functional groups of XG. It can be inferred that the isolated polysaccharides followed a similar spectral behaviour, although their biosynthesis used substrates with different MOP concentrations.

The broad absorption band at 3200–3450 cm^{-1} corresponds to the stretching vibration of hydroxyl groups (-OH) with intramolecular and intermolecular hydrogen bonds, arising from the association of alcohols and phenols. In the 15 % MOP sample, greater intensity and a small band narrowing were observed, which may indicate more specific interactions and a greater presence of hydroxyls arising from the MOP phenolic groups. The vibration at 2850–2950 cm^{-1} identified the axial deformation of C-H (absorption of symmetric and asymmetric stretching of CH_3 and CH_2 groups) and CHO; The signal around 1735 cm^{-1}, carbonyl (C═O) stretching was attributed to the esterified residues with pyruvyl (CH_3 -CO-COO) and acetyl (CH_3 -COO) and the COOH groups of glucuronic acid. Previous studies have shown that the peak attributed to the C═O vibration of acetyl groups occurs in the range of 1700–1750 cm^{-1} (Jin et al., 2015). In samples produced with MOP, there is a slight decrease in the intensity and a broadening of the peak, especially at concentrations of 15 %, 20 % and 25 %, which may indicate the favouring of intermolecular association due to partial deacetylation; the signal at 1650 cm^{-1} indicated the angular deformation of the OH bond of sugars; 1420–1430 cm^{-1}, corresponded to the C-H deflection angle; and 1050–1150 cm^{-1}, C-O axial deformation, present in all sugars. This band shows a greater intensity in the 15 % MOP group, demonstrating increased polysaccharide content (Faria et al., 2011; Pawlicka et al., 2019; Sharma and Sharma, 2023).

3.3.2. *Thermogravimetric analysis*

The derivative (DTG) curves are shown in Fig. 4 and illustrate the XG thermal decomposition steps. A first mass loss stage (30–174 °C) was observed for all samples, which was associated with disruption of the water hydrogen bonds of polysaccharide's polar groups (-OH), causing moisture desorption. According to Faria et al. (2011), XG absorbs water due to the presence of polar groups in its chemical structure. This first mass loss in the control group corresponds to a mass loss of 8.47 % (Fig. 4b), but is slightly broader than the one ascribed to XG produced in MOP-containing media.

The second thermal event observed in the control XG (181–380 °C) can be associated with the degradation of the xanthan polymer chain, which begins with the side chain groups and, subsequently, with the backbone chain unfolding (da Silva et al., 2018). A degradation stage was observed for all polymers in the range between 180 and 420 °C, associated with a loss mass of 30–40 %. This peak referred to the maximum decomposition rate of the polysaccharide.

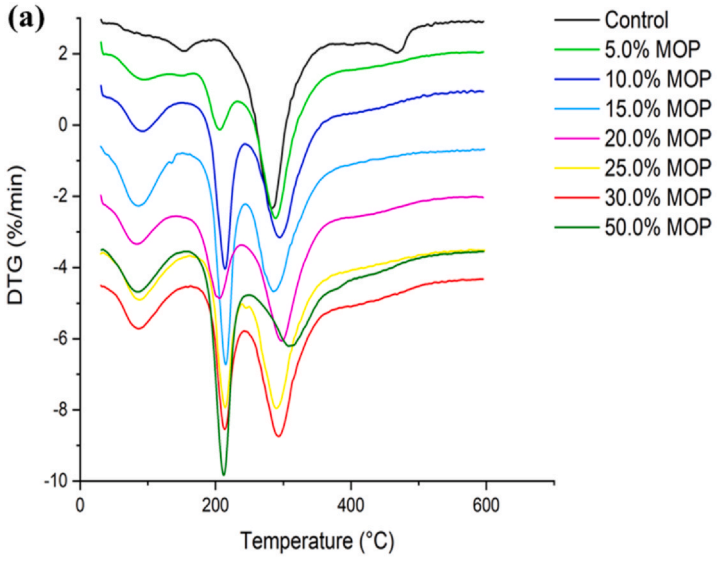

(b)

Sample	Temperature range (°C)	Mass loss (%)
Control	30-174	8.47
	181- 380	40.20
	467-550	1.21
5.0% MOP	30-127	6.46
	127-233	14.19
	233-401	36.28
10.0% MOP	30-148	9.32
	148-241	18.95
	241-403	34.36
15.0% MOP	30-150	11.40
	150-240	20.31
	241-417	34.90
20.0% MOP	30-141	11.40
	141-235	18.95
	235-402	34.89
25.0% MOP	30-163	11.00
	163-235	15.64
	242-413	32.56
30.0% MOP	30-154	11.06
	154-240	15.45
	240-393	35.54
50.0% MOP	30-155	7.94
	155-246	20.92
	246-420	30.05

Fig. 4 – Analysis of the thermal degradation of xanthan gums produced at different concentrations of MOP. (A) DTG curves of the gums (B) temperature ranges and mass loss percentage.

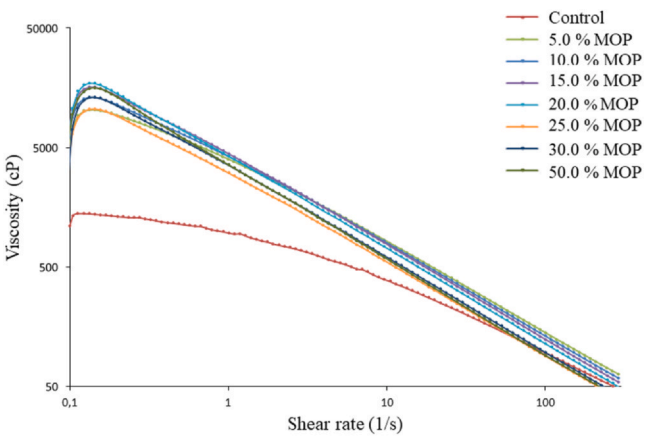

Fig. 5 – Apparent viscosity vs. shear rate of XG (aqueous solution 1 mg/mL) produced by X. campestris by introducing 5–50 % (w/v) MOP into the culture medium.

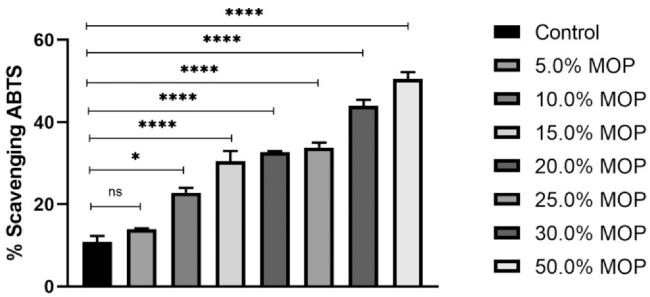

Fig. 6 – Scavenging effect of XG produced by X. campestris by introducing 5.0–50.0 % (w/v) MOP pomace into the culture medium on ABTS$^{\bullet+}$ free radicals. $^{***}p < 0.0001$; $^{*}p < 0.05$; ns = not significant.

In the XG produced in the presence of MOP, an additional mass loss with a magnitude of 14.0–21.0 % (Fig. 4b), was found at lower temperatures (127–246 °C). According to Seslija et al. (2018), the difference in the weight loss between native XG and its derivatives may be due to the presence of hydrophobic fractions in the modified samples, which decreases the retention capacity of the functional groups present MOP, under the same conditions, when compared to the unmodified polymer. On the other hand, the decomposition of modified polymers that started at relatively low temperatures may be related to the breakdown or degradation of substituent groups or weaker bonds (Sara et al., 2020). In general, the gums produced in the presence of MOP presented lower thermal stability, attributed to structural changes caused by using MOP as substrate (i.e., the second degradation stage was not observed in control). In fact, Trindade et al., (2015) found that the total or partial replacement of the sucrose carbon source by glycerol affected the structure of XG and, consequently, the thermal profile. In the control case, an additional degradation stage was observed (467–550 °C), accompanied by a mass loss of 1.21 %.

3.3.3. *Rheological behaviour*

The rheological behaviour of the produced xanthan gums, shown in Fig. 5, evidenced a typical pseudoplastic behaviour since the apparent viscosity decreased as the shear rate increased. Other authors described similar shear-thinning properties for XG (Abu Elella et al., 2021). Aiming to detect the effect of MOP use, the obtained shear stress-shear rate data were fitted to the Ostwald-de Waele model. The consistency index (*K*) and the flow behaviour index (*n*) were obtained by regression analysis, as shown in Table 1. According to this model, all the samples showed a *n* value lower than 1, confirming the pseudoplastic behaviour of the aqueous solution of these XG samples. The lowest *K* value was obtained for the control sample (878 Pa.s^n), observing a remarkable increase even when adding 5.0 % (w/v) of MOP into the production medium (3804 Pa.s^n). In fact, a progressive increase in the *K* parameter was observed with the MOP incorporation, up to 15.0 % and 20.0 % (w/v), namely the solutions with the highest consistency values. For example, the XG produced with a medium containing 15.0 % of MOP showed an increase of 395.78 % compared to the control (in addition to an increase in the production yield of 50.91 %, as discussed earlier). However, MOP concentrations above 20.0 % decreased the K parameter noticeably.

Other authors also described variations in the viscosity of XG produced under different conditions (Berninger et al., 2021). The addition of MOP impacted the molecular structure of the XG since higher *K* values are related to higher molecular weights. Larger and more ramified XG macromolecules led to more viscous solutions. Hence, higher *K* values can indicate improved polymer quality; higher molecular weights are usually desired in these types of systems (Nejadmansouri et al., 2020). The presence of acetyl groups in xanthan gum can significantly influence the conformation and properties of the macromolecule. Rheological studies carried out by Wang et al. (2022) illustrated that the gel strength and viscosity of deacetylated xanthan were higher than those of native xanthan gum. In general, acetyl groups sustain the ordered conformation of xanthan gum by maintaining the interactions between the backbone and side chains of the macromolecules. The pyruvyl concentration also influences the solutions' viscosity; in fact, xanthan gums with a higher pyruvate content usually present higher viscosity than those holding lower concentrations (Bhat et al., 2022).

In this context, adding 25.0–50.0 % of MOP had a detrimental effect on the XG macromolecule structure complexity, compared to lower dosages (i.e., lower viscosity and *K* values). This fact may be related to the effect of MOP antimicrobial (e.g., oleuropein, hydroxytyrosol and tyrosol) compounds in the metabolism of *X. campestris*.

Table 1 – Consistency index (K) and flow behaviour index (n) values obtained by fitting the experimental data shown in Fig. 5 to the Ostwald-de Waele model.

	MOP (w/v)							
	Control	5.0 %	10.0 %	15.0 %	20.0 %	25.0 %	30.0 %	50.0 %
K (Pa.s^n)	878	3804	4100	4353	4216	3009	3493	3512
n	0.6517	0.4057	0.3500	0.2939	0.2534	0.3031	0.2778	0.2445
R^2	0.97	0.98	0.98	0.99	0.98	0.98	0.99	0.99

3.4. *Antioxidant activity*

ABTS tests were performed to estimate the antioxidant potential of the produced XG samples. As shown in Fig. 6, the $ABTS^{\bullet+}$ free radicals scavenging activity of the XG increased as the MOP concentration in the medium increased (10.89; 13.96; 22.82; 30.47; 32.74; 33.85; 44.05; 50.52 % scavenging ABTS). Particularly, the identified phenolic compounds in MOP, including oleuropein, hydroxytyrosol and tyrosol, are recognised as natural antioxidants (Benavente-García et al., 2000).

XG is an anionic polysaccharide prone to establish molecular interactions to stabilise its structure, which can adopt single or double-helix conformations (Borges and Vendruscolo, 2008). Moreover, the ability of XG to interact with phenolic compounds was previously reported (Troszyńska et al., 2010). In this scenario, MOP phenolic compounds can interact by electrostatic forces with the anionic carbonyl groups of the XG, implying a molecular physical retention, thus providing antioxidant potential to the gums. This fact was particularly evidenced in the XG sample produced with 15.0 % MOP for which an increase of 179.80 % relative to the control was observed. Covalent bonds can also arise between the phenolic acids and the anionic carbonyl groups of pyruvates, enabling the biopolymer to have antioxidant properties. These effects could be responsible for the positive relationship observed between the used MOP amount and the antioxidant properties of the produced XG samples.

XG can be highlighted for its free radical reduction potential, namely the ability to inhibit lipid peroxidation and reveal a protective effect on β-glucan degradation through OH radical-induced depolymerisation (Paquet et al., 2010; Trommer and Neubert, 2005). Recent studies describe that some XG modifications can potentiate its antioxidant activity, as observed by Xiong et al. (2013), who subjected XG to hydrolysis in acid and alkaline medium, and Delattre et al. (2015) that formed a sodium salt called “xanthouronan” or xantouronan, by oxidation of xanthan with NaOCl/NaBr. In this work, producing XG in a MOP-added medium also promoted the achievement of antioxidant XG.

4. Conclusions

In this work, the biosynthesis of XG in the presence of MOP, a recalcitrant residue, was studied, showing advantages at quantitative and qualitative level. Compared to the control, the produced XG revealed a significant increase up to 30.0% MOP concentration, reaching a production increment of 50.91% ($p < 0.0001$) and a viscosity increase of 395.78% when 15.0% MOP was used. The produced biopolymers presented the XG characteristic functional groups, held a typical pseudoplastic behaviour, and improved antioxidant activity, making them interesting alternatives for high value-added applications, e.g., food, pharmaceutical and cosmetics.

Declaration of Competing Interest

The authors declare that they have no known competing financial interests or personal relationships that could have appeared to influence the work reported in this paper.

Acknowledgements

The authors are grateful to the Foundation for Science and Technology (FCT, Portugal) for financial support through national funds FCT/MCTES (PIDDAC) to CIMO (UIDB/00690/2020 and UIDP/00690/2020), and SusTEC (LA/P/0007/2021). Project OleaChain “Skills for sustainability and innovation in the value chain of traditional olive groves in the Northern Inland of Portugal” (NORTE-06-3559-FSE-000188) for P.J.L. Crugeira and A.I.G. Rodrigues contracts. FCT for the PhD research grant of H.H.S. Almeida (SFRH/BD/148124/2019). National funding by FCT, P.I., through the institutional scientific employment program contract of A. Santamaria-Echart.

References

Abu Elella, M.H., Goda, E.S., Gab-Allah, M.A., Hong, S.E., Pandit, B., Lee, S., Gamal, H., Rehman, A.U., Yoon, K.R., 2021. Xanthan gum-derived materials for applications in environment and eco-friendly materials: a review. J. Environ. Chem. Eng. Elsevier B. V. https://doi.org/10.1016/j.jece.2020.104702

Adonizio, A.L., Downum, K., Bennett, B.C., Mathee, K., 2006. Anti-quorum sensing activity of medicinal plants in southern Florida. J. Ethnopharmacol. 105, 427–435. https://doi.org/10.1016/j.jep.2005.11.025

Benavente-García, O., Castillo, J., Lorente, J., Ortuño, A., Del Rio, J.A., 2000. Antioxidant activity of phenolics extracted from Olea europaea L. leaves. Food Chem. 68, 457–462. https://doi.org/10.1016/S0308-8146(99)00221-6

Berninger, T., Dietz, N., González López, Ó., 2021. Water-soluble polymers in agriculture: xanthan gum as eco-friendly alternative to synthetics. Microb. Biotechnol. 14, 1881–1896. https://doi.org/10.1111/1751-7915.13867

Bhat, I.M., Wani, S.M., Mir, S.A., Masoodi, F.A., 2022. Advances in xanthan gum production, modifications and its applications. Biocatal. Agric. Biotechnol. 42, 102328. https://doi.org/10.1016/j.bcab.2022.102328

Bianco, M.I., Toum, L., Yaryura, P.M., Mielnichuk, N., Gudesblat, G.E., Roeschlin, R., Marano, M.R., Ielpi, L., Vojnov, A.A., 2016. Xanthan pyruvilation is essential for the virulence of Xanthomonas campestris pv. campestris. Mol. Plant-Microbe Inter. 29, 688–699. https://doi.org/10.1094/MPMI-06-16-0106-R

Böhmer-Maas, B.W., Otero, D.M., Zambiazi, R.C., Aranha, B.C., 2020. Optimization of the extraction of phenolic compounds from olive pomace using response surface methodology. Rev. Ceres 67, 181–190. https://doi.org/10.1590/0034-737x202067030003

Borges, C.D., Vendruscolo, C.T., 2008. Goma Xantana: características e condições operacionais de produção. Semin. Ciências Biológicas e da Saúde 29, 171. https://doi.org/10.5433/1679-0367.2008v29n2p171

Casadey, R., Challier, C., Altamirano, M., Spesia, M.B., Criado, S., 2021. Antioxidant and antimicrobial properties of tyrosol and derivative-compounds in the presence of vitamin B2. Assays of synergistic antioxidant effect with commercial food additives. Food Chem. 335, 127576. https://doi.org/10.1016/j.foodchem.2020.127576

Ciesielski, W., Tomasik, P., 2008. ELECTRONIC POLISH.

Cioffi, G., Pesca, M.S., De Caprariis, P., Braca, A., Severino, L., De Tommasi, N., 2010. Phenolic compounds in olive oil and olive pomace from Cilento (Campania, Italy) and their antioxidant activity. Food Chem. 121, 105–111. https://doi.org/10.1016/j.foodchem.2009.12.013

da Silva, J.A., Cardoso, L.G., de Jesus Assis, D., Gomes, G.V.P., Oliveira, M.B.P.P., de Souza, C.O., Druzian, J.I., 2018. Xanthan Gum production by Xanthomonas campestris pv. campestris IBSBF 1866 and 1867 from lignocellulosic agroindustrial wastes. Appl. Biochem. Biotechnol. 186, 750–763. https://doi.org/10.1007/s12010-018-2765-8

Dabbou, S., Dabbou, S., Selvaggini, R., Urbani, S., Taticchi, A.,

Servili, M., Hammami, M., 2011. Comparison of the chemical composition and the organoleptic profile of virgin olive oil from two wild and two cultivated Tunisian Olea europaea. Chem. Biodivers. 8, 189–202. https://doi.org/10.1002/cbdv.201000086

De M. Diniz, D., Druzian, J.I., Audibert, S., 2012. Produção de goma xantana por cepas nativas de Xanthomonas campestris a partir de casca de cacau ou soro de leite. Polimeros 22, 278–281. https://doi.org/10.1590/S0104-14282012005000032

Delattre, C., Pierre, G., Gardarin, C., Traikia, M., Elboutachfaiti, R., Isogai, A., Michaud, P., 2015. Antioxidant activities of a polyglucuronic acid sodium salt obtained from TEMPO-mediated oxidation of xanthan. Carbohydr. Polym. 116, 34–41. https://doi.org/10.1016/j.carbpol.2014.04.054

Demirci, A.S., Palabiyik, I., Apaydın, D., Mirik, M., Gumus, T., 2019. Xanthan gum biosynthesis using Xanthomonas isolates from waste bread: process optimization and fermentation kinetics. Lwt 101, 40–47. https://doi.org/10.1016/j.lwt.2018.11.018

Faria, S., De Oliveira Petkowicz, C.L., De Morais, S.A.L., Terrones, M.G.H., De Resende, M.M., De Frana, F.P., Cardoso, V.L., 2011. Characterization of xanthan gum produced from sugar cane broth. Carbohydr. Polym. 86, 469–476. https://doi.org/10.1016/j.carbpol.2011.04.063

García-Ochoa, F., Santos, V., Casas, J., Gómez, E., 2000. Xanthan gum: production, recovery, and properties. Biotechnol. Adv. 18, 549–579. https://doi.org/10.1016/S0734-9750(00)00050-1

Gunasekar, V., Reshma, K.R., Treesa, G., Gowdhaman, D., Ponnusami, V., 2014. Xanthan from sulphuric acid treated tapioca pulp: influence of acid concentration on xanthan fermentation. Carbohydr. Polym. 102, 669–673. https://doi.org/10.1016/j.carbpol.2013.11.006

Gutierrez, J., Barry-Ryan, C., Bourke, P., 2009. Antimicrobial activity of plant essential oils using food model media: efficacy, synergistic potential and interactions with food components. Food Microbiol 26, 142–150. https://doi.org/10.1016/j.fm.2008.10.008

Hahn, J., Koch, D., Niehaus, K., Ortseifen, V., 2022. Analysis of gum proteins involved in xanthan biosynthesis throughout multiple cell fractions in a “single-tube”. J. Proteom. 257, 104513. https://doi.org/10.1016/j.jprot.2022.104513

Hublik, G., 2012. Xanthan. Polym. Sci. A Compr. Ref. 10 Vol. Set 10, 221–229. https://doi.org/10.1016/B978–0-444–53349-4.00262–4.

Jin, W., Song, R., Xu, W., Wang, Y., Li, J., Shah, B.R., Li, Y., Li, B., 2015. Analysis of deacetylated konjac glucomannan and xanthan gum phase separation by film forming. Food Hydrocoll. 48, 320–326. https://doi.org/10.1016/j.foodhyd.2015.02.007

Khemakhem, I., Abdelhedi, O., Trigui, I., Ayadi, M.A., Bouaziz, M., 2018. Structural, antioxidant and antibacterial activities of polysaccharides extracted from olive leaves. Int. J. Biol. Macromol. 106, 425–432. https://doi.org/10.1016/j.ijbiomac.2017.08.037

Li, P., Li, T., Zeng, Y., Li, X., Jiang, X., Wang, Y., Xie, T., Zhang, Y., 2016. Biosynthesis of xanthan gum by Xanthomonas campestris LRELP-1 using kitchen waste as the sole substrate. Carbohydr. Polym. 151, 684–691. https://doi.org/10.1016/j.carbpol.2016.06.017

Li, X.M., Li, X.L., Zhou, A.G., 2007. Evaluation of antioxidant activity of the polysaccharides extracted from Lycium barbarum fruits in vitro. Eur. Polym. J. 43, 488–497. https://doi.org/10.1016/j.eurpolymj.2006.10.025

López, M.J., Moreno, J., Ramos-Cormenzana, A., 2001. Xanthomonas campestris strain selection for xanthan production from olive mill wastewaters. Water Res 35, 1828–1830. https://doi.org/10.1016/S0043-1354(00)00430-9

Malheiro, R., Rodrigues, N., Pereira, J.A., 2015. Olive Oil Phenolic Composition as Affected by Geographic Origin, Olive Cultivar, and Cultivation Systems, Olive and Olive Oil Bioactive Constituents. AOCS Press,https://doi.org/10.1016/B978-1-63067-041-2.50010-0

Medeiros, R.M.L., Villa, F., Silva, D.F., Júlio, L.R.C., 2016. Destinação e Reaproveitamento de Subprodutos da Extração Olivícola. Sci. Agrar. Parana. 15, 100–108. https://doi.org/10.18188/1983-1471/sap.v15n2p100-108

Mesomo, M., Silva, M.F., Boni, G., Padilha, F.F., Mazutti, M., Mossi, A., de Oliveira, D., Cansian, R.L., di Luccio, M., Treichel, H., 2009. Xanthan gum produced by Xanthomonas campestris from cheese whey: production optimisation and rheological characterisation. J. Sci. Food Agric. 89, 2440–2445. https://doi.org/10.1002/jsfa.3743

Mohsin, A., Zhang, K., Hu, J., Salim-ur-Rehman, Tariq, M., Zaman, W.Q., Khan, I.M., Zhuang, Y., Guo, M., 2018. Optimized biosynthesis of xanthan via effective valorization of orange peels using response surface methodology: a kinetic model approach. Carbohydr. Polym. 181, 793–800. https://doi.org/10.1016/j.carbpol.2017.11.076

Muscolo, A., Papalia, T., Settineri, G., Romeo, F., Mallamaci, C., 2019. Three different methods for turning olive pomace in resource: benefits of the end products for agricultural purpose. Sci. Total Environ. 662, 1–7. https://doi.org/10.1016/j.scitotenv.2019.01.210

Nejadmansouri, M., Shad, E., Razmjooei, M., Safdarianghomsheh, R., Delvigne, F., Khalesi, M., 2020. Production of xanthan gum using immobilized Xanthomonas campestris cells: effects of support type. Biochem. Eng. J. 157, 107554. https://doi.org/10.1016/j.bej.2020.107554

Pannucci, E., Caracciolo, R., Romani, A., Cacciola, F., Dugo, P., Bernini, R., Varvaro, L., Santi, L., 2021. An hydroxytyrosol enriched extract from olive mill wastewaters exerts antioxidant activity and antimicrobial activity on Pseudomonas savastanoi pv. savastanoi and Agrobacterium tumefaciens. Nat. Prod. Res. 35, 2677–2684. https://doi.org/10.1080/14786419.2019.1662006

Papagiannopoulos, A., Sotiropoulos, K., Pispas, S., 2016. Particle tracking microrheology of the power-law viscoelasticity of xanthan solutions. Food Hydrocoll. 61, 201–210. https://doi.org/10.1016/j.foodhyd.2016.05.020

Paquet, E., Turgeon, S.L., Lemieux, S., 2010. Effect of xanthan gum on the degradation of cereal β-glucan by ascorbic acid. J. Cereal Sci. 52, 260–262. https://doi.org/10.1016/j.jcs.2010.06.003

Pawlicka, A., Tavares, F.C., Dörr, D.S., Cholant, C.M., Ely, F., Santos, M.J.L., Avellaneda, C.O., 2019. Dielectric behavior and FTIR studies of xanthan gum-based solid polymer electrolytes. Electrochim. Acta 305, 232–239. https://doi.org/10.1016/j.electacta.2019.03.055

Pinheiro, A.L.B., de Almeida, P.F., Sampaio, I.C.F., Crugeira, P.J.L., dos Santos, J.N., Matos, J.B.T.L., Soares, L.G.P., Moraga Amador, D.A., Silveira, L., 2020. Effects of photo-stimulation with laser or LED on the composition of Xanthan gum produced in media containing distilled water or dialyzed or not produced water by means of Raman spectroscopy. J. Photochem. Photobiol. B Biol. 213. https://doi.org/10.1016/j.jphotobiol.2020.112057

Ramos de Souza, E., Rodrigues, P.D., Sampaio, I.C.F., Bacic, E., Crugeira, P.J.L., Vasconcelos, A.C., dos Santos Silva, M., dos Santos, J.N., Quintella, C.M., Pinheiro, A.L.B., Almeida, P.F. de, 2022. Xanthan gum produced by Xanthomonas campestris using produced water and crude glycerin as an environmentally friendlier agent to enhance oil recovery. Fuel 310, 122421. https://doi.org/10.1016/j.fuel.2021.122421

Rueda, M.P., Comino, F., Aranda, V., José Ayora-Cañada, M., Domínguez-Vidal, A., 2023. Understanding the compositional changes of organic matter in torrefied olive mill pomace compost using infrared spectroscopy and chemometrics. Spectrochim. Acta - Part A Mol. Biomol. Spectrosc. 293. https://doi.org/10.1016/j.saa.2023.122450.

Sampaio, I.C.F., Jorge Louro Crugeira, P., de Azevedo Santos Ferreira, J., Nunes dos Santos, J., Borges Torres Lima Matos, J., Luiz Barbosa Pinheiro, A., Chinalia, F.A., Fernando de Almeida, P., 2022. Up-recycling oil produced water as the media-base for the production of xanthan gum. Biopolymers 113, 1–9. https://doi.org/10.1002/bip.23488

Sara, H., Yahoum, M.M., Lefnaoui, S., Abdelkader, H., Moulai-Mostefa, N., 2020. New alkylated xanthan gum as amphiphilic derivatives: synthesis, physicochemical and rheological studies. J. Mol. Struct. 1207, 127768. https://doi.org/10.1016/j.molstruc.2020.127768

Sarangarajan, R., Meera, S., Rukkumani, R., Sankar, P., Anuradha, G., 2017. Antioxidants: friend or foe? Asian Pac. J. Trop. Med. 10, 1111–1116. https://doi.org/10.1016/j.apjtm.2017.10.017

Seslija, S., Spasojević, P., Panić, V., Dobrzyńska-Mizera, M., Immirzi, B., Stevanović, J., Popović, I., 2018. Physico-chemical evaluation of hydrophobically modified pectin derivatives: step toward application. Int. J. Biol. Macromol. 113, 924–932. https://doi.org/10.1016/j.ijbiomac.2018.03.006

Sharma, D., Sharma, P., 2023. Synergistic studies of Cassia tora gum with xanthan and guar gum: carboxymethyl synthesis of cassia gum-xanthan synergistic blend and characterization. Carbohydr. Res. 523, 108723. https://doi.org/10.1016/j.carres.2022.108723

Silva, G., de, S., Schmidt, C.A., 2015. Prospecção Tecnológica Da Produção De Goma Xantana Ao Longo Dos Anos. Cad. Prospecção 8, 92–101. https://doi.org/10.9771/s.cprosp.2015.008.011

Silva, M.F., Fornari, R.C.G., Mazutti, M.A., de Oliveira, D., Padilha, F.F., Cichoski, A.J., Cansian, R.L., Di Luccio, M., Treichel, H., 2009. Production and characterization of xantham gum by Xanthomonas campestris using cheese whey as sole carbon source. J. Food Eng. 90, 119–123. https://doi.org/10.1016/j.jfoodeng.2008.06.010

Trindade, R.A., Munhoz, A.P., Burkert, C.A.V., 2018. Impact of a carbon source and stress conditions on some properties of xanthan gum produced by Xanthomonas campestris pv. mangiferaeindicae. Biocatal. Agric. Biotechnol. 15, 167–172. https://doi.org/10.1016/j.bcab.2018.06.003

Trindade, R.A., Munhoz, A.P., Burkert, C.A.V., 2015. CARACTERIZAÇÃO DA XANTANA PRODUZIDA POR Xanthomonas campestris pv. mangiferaeindicae IBSBF 1230 UTILIZANDO DIFERENTES FONTES DE CARBONO 8, 4044–4051. https://doi.org/10.5151/chemeng-cobeq2014–0882-22847–152681.

Trommer, H., Neubert, R.H.H., 2005. The examination of polysaccharides as potential antioxidative compounds for topical administration using a lipid model system. Int. J. Pharm. 298, 153–163. https://doi.org/10.1016/j.ijpharm.2005.04.024

Troszyńska, A., Narolewska, O., Robredo, S., Estrella, I., Hernández, T., Lamparski, G., Amarowicz, R., 2010. The effect of polysaccharides on the astringency induced by phenolic compounds. Food Qual. Prefer. 21, 463–469. https://doi.org/10.1016/j.foodqual.2009.12.005

Wang, L., Xiang, D., Li, C., Zhang, W., Bai, X., 2022. Effects of deacetylation on properties and conformation of xanthan gum. J. Mol. Liq. 345, 117009. https://doi.org/10.1016/j.molliq.2021.117009

Xiong, X., Li, M., Xie, J., Jin, Q., Xue, B., Sun, T., 2013. Antioxidant activity of xanthan oligosaccharides prepared by different degradation methods. Carbohydr. Polym. 92, 1166–1171. https://doi.org/10.1016/j.carbpol.2012.10.069

Xiong, X., Li, M., Xie, J., Xue, B., Sun, T., 2014. Preparation and antioxidant activity of xanthan oligosaccharides derivatives with similar substituting degrees. Food Chem. 164, 7–11. https://doi.org/10.1016/j.foodchem.2014.05.001

Yang, Q., Cai, X., Yan, A., Tian, Y., Du, M., Wang, S., 2020. A specific antioxidant peptide: its properties in controlling oxidation and possible action mechanism. Food Chem. 327. https://doi.org/10.1016/j.foodchem.2020.126984

Zhang, Y., Zhang, C., Xu, C., Deng, Y., Wen, B., Xie, P., Huang, L., 2022. Effect of geographical location and soil fertility on main phenolic compounds and fatty acids compositions of virgin olive oil from Leccino cultivar in China. Food Res. Int. 157, 111207. https://doi.org/10.1016/j.foodres.2022.111207